Crystal Handedness and Spin Helix Chirality in $\mathbf{Fe_{1-x}Co_xSi}$

S. V. Grigoriev,[1] D. Chernyshov,[2] V. A. Dyadkin,[1] V. Dmitriev,[2] S. V. Maleyev,[1] E. V. Moskvin,[1]
D. Menzel,[3] J. Schoenes,[3] and H. Eckerlebe[4]
[1]*Petersburg Nuclear Physics Institute, Gatchina, 188300 St. Petersburg, Russia*
[2]*Swiss-Norwegian Beamlines at the European Synchrotron Radiation Facility, Grenoble, 38000 France*
[3]*Institut für Physik der Kondensierten Materie, TU Braunschweig, 38106 Braunschweig, Germany*
[4]*GKSS Forschungszentrum, 21502 Geesthacht, Germany*

(Received 2 October 2008; published 22 January 2009)

We show, with the help of polarized neutrons, that the cubic magnets $Fe_{1-x}Co_xSi$ with Dzyaloshinskii-Moriya interaction can be switched between left (for $x = 0.1$, 0.15) and right (for $x = 0.2$, 0.25, 0.3, 0.5) chiral states of the spin helix. The absolute structure was evaluated using x-ray diffraction. The crystals are shown to be enantiopure and the structural chirality changes from right handed for $x < 0.2$ to left handed for $x > 0.2$. These compounds are compared with the etalon sample of MnSi which is identified as having the left-handed chirality both in the magnetic and crystallographic sense.

DOI: 10.1103/PhysRevLett.102.037204 PACS numbers: 75.25.+z, 61.05.cp, 61.05.fg, 75.50.Bb

The chirality, determined as an asymmetry of the object upon its mirroring, plays an important and sometimes dramatic role in biology, chemistry, and physics. Alice, when she jumped through the looking glass in her adventure, discovered a world with completely different, sometimes opposite properties. In reality, unlike in Alice's dreams, the step through "the looking glass" is somewhat more difficult. It is, therefore, of great importance, first, to reveal the fundamental forces underlaying the chirality as a phenomenon and, second, to control the chirality of an object.

One example of chiral objects in solid state physics are noncentrosymmetric cubic magnets with the space group $P2_13$, such as MnSi, FeGe, and $Fe_{1-x}Co_xSi$, etc. Handedness of the atomic configuration of the series of MnSi, FeSi, CoSi, and $Fe_{0.5}Co_{0.5}Si$ has been examined long ago [1] by convergent beam electron diffraction. Surprisingly, the same chiral configurations were found in all these crystals although both left- and right-handed systems should have the same formation energy. For example, quartz crystals are known to realize the left- and/or the right-handed enantiomers [2].

Furthermore, these compounds are magnetically ordered in a one-handed spin helical structure with the very long period of 10–100 nm [3–6]. The spin helicity is a result of the equilibrium between the ferromagnetic exchange interaction and the antisymmetric Dzyaloshinskii-Moriya (DM) interaction caused by the lack of a center of symmetry in the atomic arrangement [7–9]. A weak anisotropic exchange (AE) interaction tends to fix the direction of the helix along principal cube directions: either $\langle 111\rangle$, or $\langle 100\rangle$ axes [8].

The intuitive supposition, that the crystallographic chirality sets rigorously the sign of the DM interaction and, therefore, the sense of the magnetic chirality, was not confirmed experimentally. According to [1,4] the left-handed atomic configuration found in MnSi corresponds to the left-handed helix chirality. On the contrary, the reported left-handed crystallographic chirality of the $Fe_{1-x}Co_xSi$ with $x = 0.2$, 0.4, and 0.5 [1] coexists with a right-handed helicity [4]. Despite the fundamental importance of understanding chirality, these distinctive experimental results have not been revisited for more than 20 years.

In this Letter we report on new structural and magnetic data for $Fe_{1-x}Co_xSi$ that shed light on the more than 20-year-old puzzle. Nowadays, the absolute structure and its chiral configuration can be readily determined by properly collected single crystal diffraction data [10,11], and magnetic helicity can be almost routinely characterized with polarized neutrons [12]. We have combined these two experimental techniques to show that the spin helix chirality changes together with the structural chirality as a function of Co doping.

As is well known, the mixed crystals $Fe_{1-x}Co_xSi$ order below T_C in a one-handed helical spin structure with a small propagation vector $k < 0.025$ Å^{-1} in the concentration range $0.05 < x < 0.80$ [5,6,13]. High-purity single crystals of MnSi and $Fe_{1-x}Co_xSi$ with $x = 0.1$, 0.15, 0.20, 0.25, 0.30, and 0.50, grown by the Chokhralski method were chosen for this study. They were disks with diameter of the order of 8 mm and thickness of the order of 1 mm. The polarized small-angle neutron diffraction measurements were performed with the help of the SANS2 instrument at the GeNF. A neutron beam with initial polarization $P_0 = 0.93$, with mean wavelength of $\lambda = 0.58$ nm ($\Delta\lambda/\lambda = 0.1$) was used. A weak magnetic field (1 mT) guiding the polarization was applied perpendicularly to the incident neutron beam.

The polarized neutron diffraction is known as an ideal tool for measuring spin chirality [12]. The pure magnetic elastic cross section of the polarized neutrons consists of polarization-independent and polarization-dependent contributions. The latter is also asymmetric with respect to the momentum transfer $\mathbf{Q}$ and associated with the average chirality of the magnetic system. It can be determined by measuring the difference between the scattering intensities taken from the incident neutron beam with the polarization along ($+P_0 = \mathbf{P}_0 \cdot \mathbf{h}$) and opposite ($-P_0 = \mathbf{P}_0 \cdot \mathbf{h}$) to the guiding magnetic field $\mathbf{h}$ at the fixed position in the momentum space $\mathbf{Q} = \mathbf{k}$. To quantify the helix chirality we introduce the value P_s (the difference between two intensities at the same $\mathbf{Q}$ normalized to their sum) which has a simple relation to the measure of the helix chirality γ of the system [14]:

$$P_s(\mathbf{Q}) = \frac{I(+\mathbf{P}_0) - I(-\mathbf{P}_0)}{I(+\mathbf{P}_0) + I(-\mathbf{P}_0)} = \gamma(\mathbf{P}_0 \cdot \mathbf{e}_Q) = \gamma P_0 \cos\psi, \tag{1}$$

where ψ is the angle between the polarization vector $\mathbf{P}_0$ and the unit scattering vector $\mathbf{e}_Q$. Using the position-sensitive detector in the small-angle diffraction measurements one is able to record in one shot the scattering intensity at two distinct Bragg reflections $\mathbf{Q} = \mathbf{k}$ and $\mathbf{Q} = -\mathbf{k}$. Figure 1 shows a typical map of SANS intensity from the MnSi sample at temperature $T = 25$ K with the polarization along $+\mathbf{P}_0$ (a) and opposite $-\mathbf{P}_0$ (b) the magnetic field. Since MnSi is known to show the left-handed helix and the left-handed crystallographic configuration [3], this sample and the corresponding scattering maps are considered an etalon for other measurements. The γ ratio for this sample was obtained to be equal to 1 ± 0.01 in the whole range $T < T_C$ [14].

Figure 2 shows the maps of the polarized SANS intensities with the polarization along the field $+P_0$ for four different samples of the $\mathrm{Fe}_{1-x}\mathrm{Co}_x\mathrm{Si}$ system with $x = 0.10$ (a), $x = 0.15$ (b), $x = 0.20$ (c), $x = 0.25$ (d) at $T = 9$ K, i.e., below $T_c(x)$. Comparing the map with $+P_0$ of MnSi [Fig. 1(a)] with those of $\mathrm{Fe}_{1-x}\mathrm{Co}_x\mathrm{Si}$ one can see that, similarly to MnSi, the samples with $x = 0.1$ and 0.15 [Figs. 2(a) and 2(b)] show maxima of the scattering intensity on the left side of the detector. This means that these three compounds have the same left-handed chirality of the helices. On the contrary, the other two compounds with $x = 0.2, 0.25$ [Figs. 2(c) and 2(d)] show scattering maxima on the right side of the detector, implying that they have a chirality opposite to MnSi, i.e., they are right handed. The other samples (not shown in the figures) with $x = 0.30$ and 0.50 reveal a scattering similar to that for $x = 0.20, 0.25$, i.e., they are identified as being right handed in agreement with reported data [1,4].

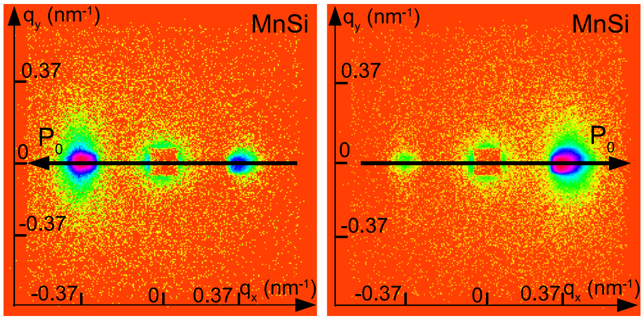

FIG. 1 (color online). Maps of the polarized SANS intensities of MnSi for the polarization $\mathbf{P}_0$ along the guide field (left) and opposite to it (right) at $T = 25$ K.

According to the Bak-Jensen model [8], the helix wave vector $\mathbf{k}$ is the key parameter in the description of the magnetic structure of these compounds. Its length $k = S|\mathbf{D}|/A$ is the ratio between the DM constant $|\mathbf{D}|$ and the exchange constant (spin wave stiffness) A. S is the average spin per unit cell. The sign of the wave vector $\mathbf{k}$ determines the chirality of the helical structure and is directly connected to the sign of the Dzyaloshinskii constant sgn($\mathbf{D}$). The orientation of $\mathbf{k}$ in the Q space is determined by the anisotropic spin-orbit interaction, which pins the helix along one of the principal directions.

The wave vector $\mathbf{k}$ (in its length, its sign, and its direction) demonstrates a drastic change with the concentration at $x \sim 0.2$. First, the chirality, which is connected to the sign of the wave vector, is flipped at $x \sim 0.2$ (Fig. 3). Second, the value of the wave vector k increases with the increase of x for $x < 0.2$ and decreases smoothly for $x > 0.2$ (Fig. 3). Third, as shown in Fig. 2, the direction of the wave vector $\mathbf{k}$ changes. In $\mathrm{Fe}_{0.90}\mathrm{Co}_{0.10}\mathrm{Si}$ the helix wave vector $\mathbf{k}$ is definitely oriented along the [100] axis

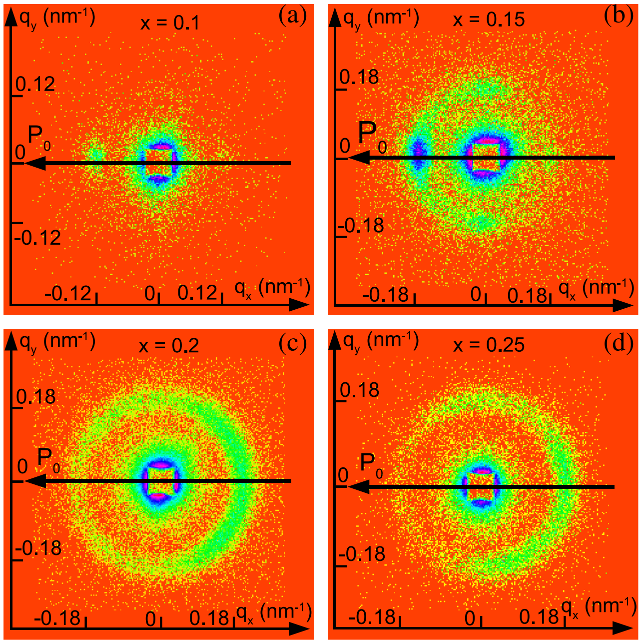

FIG. 2 (color online). Maps of the polarized SANS intensities for $\mathbf{P}_0$ along the guide field of $\mathrm{Fe}_{1-x}\mathrm{Co}_x\mathrm{Si}$ with $x = 0.10$ (a), $x = 0.15$ (b), $x = 0.20$ (c), $x = 0.25$ (d). The maps (a) and (b) show the left chirality, but samples at (c) and (d) are right handed.

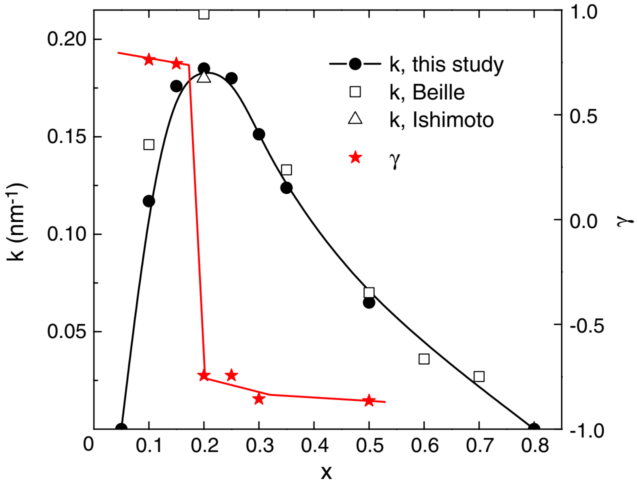

FIG. 3 (color online). Dependence of the helix wave vector k and the chirality γ on the Co concentration x for $Fe_{1-x}Co_xSi$ (□ [5], △ [6], ● this study).

[Fig. 2(a)], which is set along the direction of polarization. In $Fe_{0.85}Co_{0.15}Si$ the spiral wave vector **k** is oriented along the [100] and [010] axes but the scattering intensity is slightly blurred [Fig. 2(b)], indicating some distribution of the **k** orientation. With a further increase of the Co concentration the peaks become strongly blurred with a clear tendency to form a ring of the radius $|\mathbf{k}|$ in the intensity map. In $Fe_{1-x}Co_xSi$ with $x = 0.2$, 0.25 [Figs. 2(c) and 2(d)], and $x = 0.30$, 0.5 (not shown) the spiral wave vector **k** is almost randomly oriented. The quasirandom distribution of the k vector is obviously linked to the distortion that Co doping introduces to the system. This distortion changes the character of the anisotropy and makes it local compared to the scale of the spiral period. One should distinguish between the orientation of the wave vector **k**, which can be any for randomly oriented helix domains, and the chirality γ, which can be the same for all these domains. For example, the sum of two intensities $\Sigma = I(\mathbf{Q}, +\mathbf{P}_0) + I(\mathbf{Q}, -\mathbf{P}_0)$ gives the pattern of scattering for nonpolarized neutrons. The values of Σ at $|\mathbf{Q}| = |\mathbf{k}|$ are shown in Fig. 4 as a function of the azimuth angle ψ taken anticlockwise from the horizontal axis for the compound with $x = 0.2$. The intensity of the ring at $|\mathbf{Q}| = |\mathbf{k}|$ changes with the angle ψ, showing an almost random distribution of the wave vector orientation. P_s varies in accordance with Eq. (1) with the cosine of ψ (Fig. 4). The amplitude is equal to γP_0, from which the chirality γ of the system can be determined unambiguously. In conclusion, the increase of the Co concentration results in a transition of the magnetic structure from the left-handed helix for $x < 0.2$ with the preferable orientation along the [100] axis to the right-handed helix for $x \geq 0.2$ with a random orientation of **k**.

X-ray diffraction of single crystals under certain conditions also allows one to distinguish between left- and right-handed enantiomorphs. The corresponding technique based on the Flack parameter [10] has been applied to many compounds and is routinely used by crystallographers. As in the case for neutron scattering, we illustrate only the main idea. The Flack parameter f can be expressed via half-difference of intensities of Friedel equivalents [10,11]:

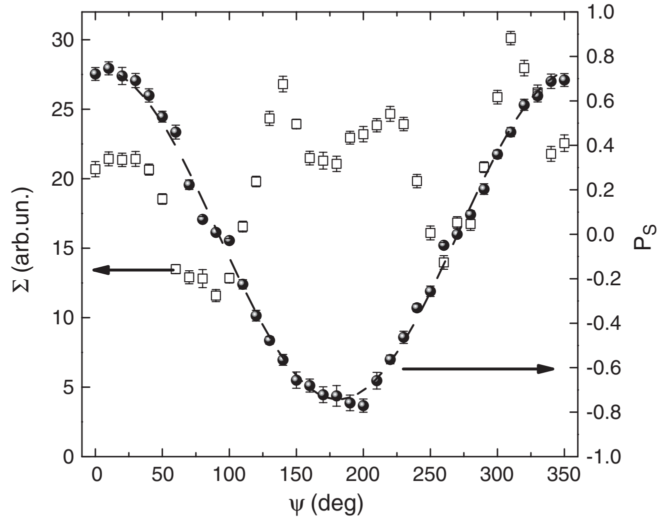

FIG. 4. Dependence of the scattering intensity Σ and the value P_s on the azimuth angle ψ seen anticlockwise from the horizontal axis for the compound with $x = 0.2$.

$$I(\mathbf{H}) - I(-\mathbf{H}) = (1 - 2f)[|F(\mathbf{H})|^2 - |F(-\mathbf{H})|^2]. \quad (2)$$

Here I and F denote the intensity and the structural factor for the Bragg reflection **H**, respectively. The Flack parameters may, therefore, be considered a measure of the ratio of domains of different handedness. A zero value of Flack parameter indicates an enantiopure sample with the correct absolute structure. For a Flack parameter equal to 1 the crystal structure has to be inverted. The ability of the x-ray diffraction experiment to distinguish between structures with opposite chirality originates from the resonance scattering contribution in the structural amplitudes. This contribution defines the wavelength-dependent inversion-distinguishing power (IDP) [11], $|F(\mathbf{H})|^2 - |F(-\mathbf{H})|^2$. A simple estimation reveals that a wavelength $\lambda = 0.77$ Å provides sufficient IDP for many Bragg reflections.

The x-ray diffraction data were collected with synchrotron radiation with $\lambda = 0.77$ Å at the Swiss-Norwegian Beam Line BM1A at the ESRF (Grenoble, France) using the KUMA6 diffractometer. Crystals with an average size about 50 μm were prepared from the same batches as used for the neutron scattering measurements. The absolute structure was found by refining the Flack parameter [10], together with the inspection of the inverted structure. The structure of the etalon MnSi sample is identical to those found in the literature [3], with $u_{Mn} = 0.135$ and $u_{Si} = 0.845$.

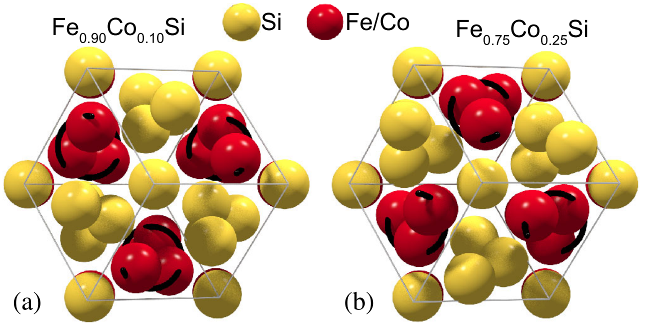

FIG. 5 (color online). The view of the B20 structure along the (111) axis for the sample with $x = 0.10$ (a) and $x = 0.25$ (b). The chirality of the metal sublattice is left handed for $x = 0.10$ and right handed for $x = 0.25$. The black spirals help to identify the sense of the skewing.

The structure of the compound with $x = 0.10$ is identified as $P2_13$ with the structural parameters $u_{\mathrm{Fe\ or\ Co}} = 0.863$ and $u_{\mathrm{Si}} = 0.157$. For the compound with $x = 0.25$, $u_{\mathrm{Fe\ or\ Co}} = 0.112$, and $u_{\mathrm{Si}} = 0.407$. Low R factors ($x = 0.10$, $R_1 = 1.8\%$, $wR = 3.8\%$; and $x = 0.25$, $R_1 = 1.7\%$, $wR = 4.3\%$) together with a well-defined Flack parameter of the order of 0.00(6) confirm that the absolute structure has been determined correctly. With the absolute structure the crystallographic chirality of a helix propagating along a given direction can easily be determined. Figure 5 shows the view of the B20 structure viewed along the (111) axis for the sample with $x = 0.10$ (a) and $x = 0.25$ (b). The Fe or Co atoms forming a helix [not laying on the (111) axis] are skewing around it in the certain left-handed configuration for $x = 0.10$ and in the right-handed configuration for $x = 0.25$. The coordinates on pure MnSi give the very clear right-handed structure of the Mn sublattice identical to that shown in Fig. 5(b) for $x = 0.25$.

Thus, we conclude that the change of handedness observed in the magnetic structure is coherent with the change in crystallographic absolute structure. A comparison of the left-handed structure for $x = 0.10$ with the right-handed one for $x = 0.25$ shows that there are not simply left and right domains of the same structure, but rather two close structures differing by handedness and also by a shift along the [111] axis. This small difference in structure correlates with and probably determines qualitatively and quantitatively the different magnetic properties of $Fe_{1-x}Co_xSi$ (Fig. 3).

Interestingly, the ratio between structural and magnetic chirality is different for the compounds (right-left for MnSi) and (left-left, or, right-right for $Fe_{1-x}Co_xSi$). This difference can be interpreted on the basis of a deep connection between the magnetic and transport properties of these compounds, which was recently demonstrated [15]. The presence of the anomalous Hall effect, in contrast to its absence in MnSi, favors the itinerant nature of magnetism in $Fe_{1-x}Co_xSi$ [15]. The positive temperature-independent magnetoresistance in $Fe_{1-x}Co_xSi$ is again opposite to that in MnSi, where it is negative and temperature dependent [15]. Thus, the itinerant electron systems differently interact with the lattice structure, which is also reflected in the magnetic chirality, and therefore in the sign of the DM interaction.

In conclusion, we give experimental evidence for the flip of the spin helix chirality along with the structural chirality of the Fe sublattice in $Fe_{1-x}Co_xSi$, from left handed at $x < 0.2$ to right handed at $x \geq 0.2$. This correlation is not a fortunate coincidence, but an indication that the sign of the Dzialoshinskii-Moriya interaction, which determines the handedness of the magnetic spiral, is a function of the atomic arrangement. A comparison with MnSi shows that there is another factor related to the specific character of the itinerancy, which is able to change the helix chirality along with the sign of the Dzialoshinskii-Moriya interaction. Our findings open new possibilities for controlling the spin chirality not only in $Fe_{1-x}Co_xSi$ but also in the other ternary mixed compounds based on the B20 structure.

The PNPI-team acknowledges the GKSS for their hospitality. The work is supported in part by the RFBR (Project No 07-02-01318).

[1] M. Tanaka, H. Takayoshi, M. Ishida, and Ya. Endoh, J. Phys. Soc. Jpn. **54**, 2970 (1985).
[2] Y. Tanaka *et al.*, Phys. Rev. Lett. **100**, 145502 (2008).
[3] Y. Ishikawa *et al.*, Solid State Commun. **19**, 525 (1976); Y. Ishikawa *et al.*, Phys. Rev. B **16**, 4956 (1977).
[4] M. Ishida, Ya. Endoh, S. Mitsuda, Yo. Ishikawa, and M. Tanaka, J. Phys. Soc. Jpn. **54**, 2975 (1985).
[5] J. Beille *et al.*, Solid State Commun. **47**, 399 (1983); J. Beille *et al.*, J. Phys. F **11**, 2153 (1981).
[6] K. Ishimoto *et al.*, J. Magn. Magn. Mater. **90–91**, 163 (1990); K. Ishimoto *et al.*, Physica (Amsterdam) **213B–214B**, 381 (1995).
[7] I. E. Dzyaloshinskii, Zh. Eksp. Teor. Fiz. **46**, 1420 (1964).
[8] P. Bak and M. H. Jensen, J. Phys. C **13**, L881 (1980).
[9] D. Nakamishi, A. Janase, A. Hasejawa, and M. Kitaoka, Solid State Commun. **35**, 995 (1980).
[10] H. D. Flack, Acta Crystallogr. Sect. A **39**, 876 (1983).
[11] H. D. Flack, Acta Crystallogr. Sect. A **55**, 908 (1999).
[12] S. V. Maleyev, Phys. Rev. Lett. **75**, 4682 (1995).
[13] S. V. Grigoriev *et al.*, Phys. Rev. B **76**, 092407 (2007); S. V. Grigoriev *et al.*, Phys. Rev. B **76**, 224424 (2007).
[14] S. V. Grigoriev *et al.*, Phys. Rev. B **74**, 214414 (2006).
[15] N. Manyala *et al.*, Nature (London) **404**, 581 (2000); N. Manyala, Y. Sidis, J. F. DiTusa, G. Aeppli, D. P. Young, and Z. Fisk, Nature Mater. **3**, 255 (2004).